Synthesis and phase transition of negative thermal expansion materials $Zr_{1-x}Lu_xW_2O_{8-y}$

Yasuhisa Yamamura*, Masayuki Kato, Toshihide Tsuji

*School of Materials Science, Japan Advanced Institute of Science and Technology, 1-1 Asahidai,
Tatsunokuchi, Ishikawa 923-1292, Japan*

Abstract

$Zr_{1-x}Lu_xW_2O_{8-y}$ solid solutions were newly synthesized by a solid sate reaction method. X-ray diffraction (XRD) experiments from 90 to 560 K revealed that the solid solutions were of a single phase up to $x = 0.04$ and showed a negative thermal expansion. Order–disorder phase transition temperatures (T_{trs}) and saturated order parameters (η_s) associated with WO_4 orientational order were determined from the XRD results. The linear relationship between the normalized T_{trs} and η_s obtained for $Zr_{1-x}M_xW_2O_{8-y}$ (M = Sc, Y, In) in our previous study was also found for $Zr_{1-x}Lu_xW_2O_{8-y}$. A heat capacity anomaly due to the order–disorder phase transition was detected for $Zr_{0.96}Lu_{0.04}W_2O_{8-y}$ by a relaxation calorimeter. T_{trs} of the solid solutions drastically decreased with increasing Lu content. The drastic suppression of T_{trs} can be explained by the model assuming the existence of a local nano-region including the WO_4 pairs having the orientational disorder.
© 2005 Elsevier B.V. All rights reserved.

Keywords: Negative thermal expansion; Order–disorder phase transition; ZrW_2O_8

1. Introduction

ZrW_2O_8 consists of ZrO_6 octahedra and WO_4 tetrahedra, and shows an isotropic shrinkage on heating, the so-called isotropic negative thermal expansion, over a wide temperature region of 1000 K [1,2]. Although its thermal expansion coefficient is negative over the whole temperature range, there is a small discontinuity around 440 K. This is due to an order–disorder phase transition associated with the orientation of the unshared vertex of WO_4 tetrahedron. The structural [1,2] and thermodynamic [3,4] considerations revealed that the WO_4 pair, which consists of two WO_4 tetrahedra lying in tandem on the [1 1 1] body diagonal line in a unit cell, has only two configurations and changes their orientations concertedly. That is, the phase transition of ZrW_2O_8 can be described with the 3D-Ising model, where one pair of the adjacent two WO_4 tetrahedra behaves just like an Ising-spin [5].

In our previous studies [6–8], the phase transition temperature of ZrW_2O_8 was affected strongly by some trivalent cations substituted for Zr sites. The phase transition temperature (T_{trs}) of $Zr_{1-x}M_xW_2O_{8-y}$ (M = Sc, Y, In) decreased drastically with the increase of just a few percent in M content. Especially, the depression in T_{trs} amounts to 80 K (approximately 20%) in $Zr_{0.96}Sc_{0.04}W_2O_{8-y}$ [6]. To explain the effect of the substitution by the trivalent cation in ZrW_2O_8, we previously proposed a model that the substituted trivalent cation forms a small region which is frozen into the glassy state with the orientational disorder of WO_4 and keeps the structure of high-temperature phase [7]. The small regions behave just like nonmagnetic impurities in a site-diluted magnetic system, leading to the drastic decrease of the phase transition temperature in $Zr_{1-x}M_xW_2O_{8-y}$ (M = Sc, Y, In). This model can explain the substitution effect on $Zr_{1-x}M_xW_2O_{8-y}$

---

* Corresponding author. Present address: Department of Chemistry, Graduate School of Pure and Applied Sciences, University of Tsukuba, Tsukuba, Ibaraki 305-8571, Japan. Tel.: +81 29 853 5600x8243; fax: +81 29 853 6503.

E-mail address: yasu@chem.tsukuba.ac.jp (Y. Yamamura).

(M = Sc, Y, In) very well. In order to see if the model applies to another solid solution substituted by rare earth element having 4f electrons, $Zr_{1-x}Lu_xW_2O_{8-y}$ solid solution was newly synthesized in the present study.

2. Experimental

The samples of $Zr_{1-x}Lu_xW_2O_{8-y}$ ($x = 0.02$, 0.04) were synthesized by a solid state reaction method. Starting materials were ZrO_2 (Nakarai Tesque., high purity), WO_3 (Kojiundo Chemical Lab, 99.99%) and Lu_2O_3 (Kojiundo Chemical Lab, 99.99%). These materials were mixed in an agate mortar and pressed into pellets. The pellets were sintered in air at 1473 K for 20 h and quenched in liquid nitrogen. All samples were characterized by X-ray diffractometer using Cu Kα radiation with 40 kV–200 mA (RINT 2500V, Rigaku), having a low temperature attachment capable of controlling temperature within ±1 K. The X-ray powder diffraction (XRD) data were collected by a step scanning method in the 2θ range from $10°$ to $100°$. The power patterns were obtained in a vacuum from 90 to 560 K, where temperature was kept at constant at each temperature. After XRD measurements, the surface temperature of the sample was calibrated against the system temperature by using another K-type thermocouple attached directly on the surface of the sample, and then a correction curve of sample temperature was calculated. These collected temperatures were used as the sample temperature in these experiments. Heat capacity of $Zr_{0.96}Lu_{0.04}W_2O_{8-y}$ was measured from 230 to 400 K by a commercial relaxation calorimeter (Quantum Design PPMS). The prepared sample (10.9133 mg) was contacted to the sample holder with Apiezon-H grease.

3. Results and discussion

The X-ray diffraction patterns of the prepared samples $Zr_{1-x}Lu_xW_2O_{8-y}$ ($x = 0.02$, 0.04) at room temperature are depicted in Fig. 1, together with that of ZrW_2O_8 [8]. They
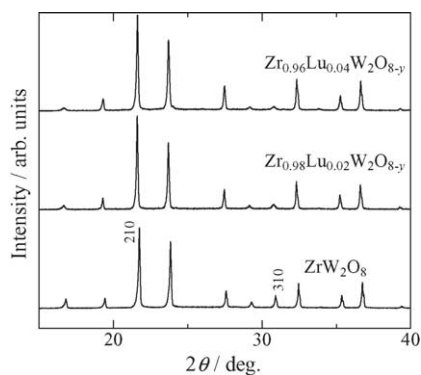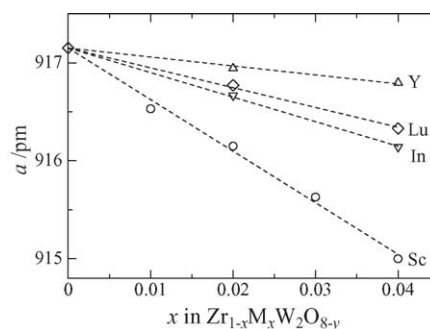
Fig. 2. Lattice parameters of $Zr_{1-x}Lu_xW_2O_{8-y}$ ($x = 0$, 0.02, 0.04), together with those of $Zr_{1-x}M_xW_2O_{8-y}$ (M = Sc, Y, In) at 121 K [6].

were confirmed to be of a single phase having the same cubic crystal structure as ZrW_2O_8. Their lattice parameters were determined using about 30 diffraction peaks between $40°$ and $100°$ by a least-squares method after correcting 2θ with Nelson–Rieley's method [9]. The lattice parameters of $Zr_{1-x}Lu_xW_2O_{8-y}$ at 121 K, which was much lower than the order–disorder phase transition temperatures, are plotted against Lu content in Fig. 2, together with those of $Zr_{1-x}M_xW_2O_{8-y}$ (M = Sc, Y, In) [6]. The lattice parameter of $Zr_{1-x}Lu_xW_2O_{8-y}$ decreased linearly with increasing Lu content. The linearity of the lattice parameter against Lu content fulfills Vegard's law and ensures that $Zr_{1-x}Lu_xW_2O_{8-y}$ forms a solid solution at least up to $x = 0.04$. The lattice parameters of the solid solutions are smaller than that of ZrW_2O_8, though the ionic radius of substituted Lu^{3+} ions is larger than that of Zr^{4+} [10]. This reduction was seen also in the system of $Zr_{1-x}M_xW_2O_{8-y}$ (M = Sc, Y, In).

Fig. 3 shows the temperature dependence of the lattice parameter in $Zr_{1-x}Lu_xW_2O_{8-y}$, together with that of ZrW_2O_8 [4]. The solid solutions contract with increasing temperature. A slope of lattice parameter as a function of temperature corresponds to a thermal expansion coefficient in a crystal. The coefficients of $Zr_{1-x}Lu_xW_2O_{8-y}$ are negative over the measuring temperature region in this study. There are, however, slight changes of the coefficients on the lattice parameters of the solid solutions between 350 and 400 K. They are attributed to the order–disorder phase transition associated to
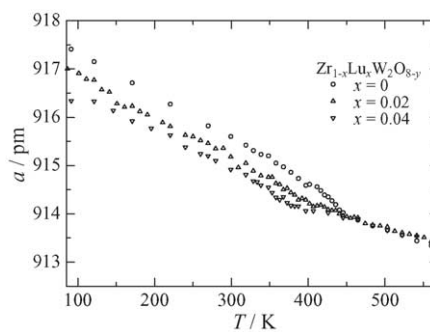
Fig. 1. X-ray diffraction patterns of $Zr_{1-x}Lu_xW_2O_{8-y}$ ($x = 0.02$, 0.04) at room temperature, together with ZrW_2O_8 [8].

Fig. 3. Lattice parameters of $Zr_{1-x}Lu_xW_2O_{8-y}$ ($x = 0$, 0.02, 0.04) as a function of temperature.
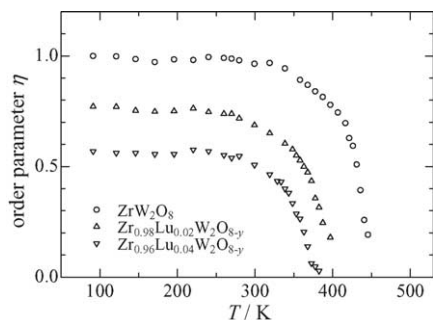
Fig. 4. Temperature dependence of order parameter in $Zr_{1-x}Lu_xW_2O_{8-y}$ ($x = 0, 0.02, 0.04$).

disordering of WO_4 orientation, considering the behavior of ZrW_2O_8.

The low temperature phase of ZrW_2O_8 has some characteristic diffraction peaks, e.g., 310 and 111 superlattice reflections, whose intensities decrease with increasing temperature and disappear above the phase transition temperature (T_{trs}). Since the square root of the integrated intensity is proportional to crystal structure factor, that of the 310 reflection corresponds to a degree of order associated with the orientation of WO_4 pairs in ZrW_2O_8. Upon cooling, the integrated intensity increases from zero to a saturated value at sufficiently low temperatures below T_{trs}. If the integrated intensity is normalized by the saturated value at very low temperature, its change from zero to unity can be regarded as a so-called order parameter of the order–disorder phase transition assuming the complete order at low temperature. In the previous work [7], we introduced the order parameter, η, as the following equation:

$$\eta = \sqrt{\frac{\{(I_{310}/I_{210})_{Zr_{1-x}M_xW_2O_{8-y}}\}_T}{\{(I_{310}/I_{210})_{ZrW_2O_8}\}_{\text{saturated}}}},$$

where I_{310} is the integrated intensity of the 310 diffraction peak and I_{210} the integrated one of the 210 diffraction peak, which is the largest fundamental peak, to normalize the integrated peak intensity. The denominator is the saturated (I_{310}/I_{210}) value of ZrW_2O_8. The saturated η of ZrW_2O_8 can be regarded to be a unity, because ZrW_2O_8 shows the effectively complete order [5]. Here, influence of preferred orientation of crystal upon the order parameter is negligible in the present case, because ZrW_2O_8 shows cubic structures in both the low- and the high-temperature phases.

Fig. 4 shows the order parameters of $Zr_{1-x}Lu_xW_2O_{8-y}$ as a function of temperature. These η of $Zr_{1-x}Lu_xW_2O_{8-y}$ are saturated below about 200 K to a smaller magnitude than that of the mother compounds. This means that the orientational order in solid solutions is not perfect even at low temperature. The order parameter decreases from the saturated values with increasing temperature and finally disappears at the transition temperature. This temperature dependence of $Zr_{1-x}Lu_xW_2O_{8-y}$ substituted by rare earth element having 4f electrons is in similar to those of

$Zr_{1-x}M_xW_2O_{8-y}$ (M = Sc, Y, In) reported in our previous study [6].

The order–disorder phase transition temperatures of $Zr_{1-x}Lu_xW_2O_{8-y}$ ($x = 0.02, 0.04$) were determined as the temperature where η disappeared by using extrapolating the η curve to zero value. The phase transition temperatures (T_{trs}) of $Zr_{1-x}Lu_xW_2O_{8-y}$ are plotted in Fig. 5 as a function of substituted Lu content. The T_{trs} of $Zr_{1-x}Lu_xW_2O_{8-y}$ decreases linearly with increasing Lu content. This linearity of the composition dependence of T_{trs} was seen also in those of $Zr_{1-x}M_xW_2O_{8-y}$ (M = Sc, Y, In) [6]. In the $Zr_{1-x}M_xW_2O_{8-y}$ system, the T_{trs} of the 4%-substituted solid solution decreased in order of Y (394 K), In (377 K), Lu (373 K) and Sc (363 K) [6].

The heat capacity measurement was carried out firstly for $Zr_{0.96}Lu_{0.04}W_2O_{8-y}$ substituted by trivalent cation from 200 to 390 K. The obtained heat capacity is depicted in Fig. 6(a). The heat capacity seems to be a smooth curve apparently around the T_{trs} of $Zr_{0.96}Lu_{0.04}W_2O_{8-y}$ (373 K) estimated from the X-ray study, though the heat capacity of ZrW_2O_8 has a large and sharp anomaly around the phase transition temperature [11]. To clarify its temperature dependence, the equivalent Debye temperature corresponding to the heat capacity is estimated and depicted in Fig. 6(b). It is found that there was a small anomaly due to the order–disorder phase transition around 370 K. The anomaly in the heat capacity of $Zr_{0.96}Lu_{0.04}W_2O_{8-y}$ is much smaller than that of ZrW_2O_8 [11]. This fact can be related to the small saturated order parameter, η_s, of $Zr_{0.96}Lu_{0.04}W_2O_{8-y}$ as shown in Fig. 4. The saturated order parameter corresponds to the number of WO_4 pairs that contribute to the order–disorder phase transition. To estimate enthalpy and entropy of transition, we need a normal heat capacity to separate an excess heat capacity. In the case of ZrW_2O_8, the excess heat capacity contributes to the range over about 300 K [11]. Since the present heat capacity measurement was carried out in the narrow temperature region, we were not able to estimate the normal heat capacity in this study.

Fig. 7 shows the saturated order parameters, η_s, of $Zr_{1-x}Lu_xW_2O_{8-y}$ as a function of Lu content. The decrease in the η_s means the reduction of the number of the WO_4 pairs with the ordered orientation. In other words, some local
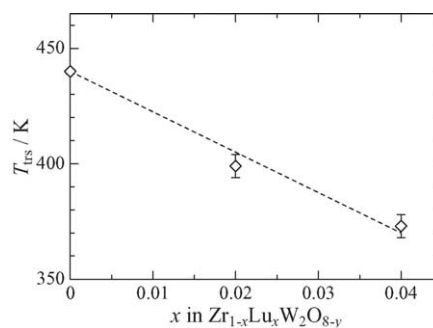

Fig. 5. Order–disorder phase transition temperatures of $Zr_{1-x}Lu_xW_2O_{8-y}$ ($x = 0, 0.02, 0.04$) against Lu content.
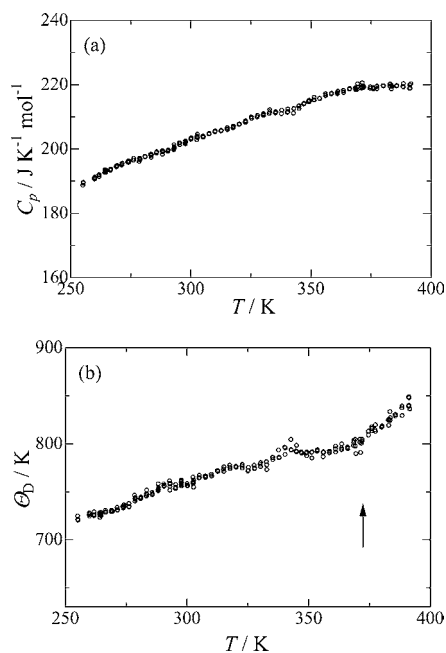
Fig. 6. (a) Heat capacity of $Zr_{0.96}Lu_{0.04}W_2O_{8-y}$; (b) equivalent Debye temperature (assuming 32.94 degrees of freedom per the chemical formula of $Zr_{0.96}Lu_{0.04}W_2O_{7.98}$) corresponding to the heat capacity of $Zr_{0.96}Lu_{0.04}W_2O_{8-y}$. A depression around 370 K in (b) is due to the order–disorder phase transition.

regions including the WO_4 pairs with the orientational disorder are generated in the crystal by the substitution. Indeed, this situation was confirmed by broadening of the full width at half maximum (FWHM) of the 310 superlattice peak in $Zr_{1-x}Lu_xW_2O_{8-y}$, through the detailed analysis of the diffraction patterns in Fig. 1. This broadening of the FWHM results from the disturbance of the periodic order by some clusters including some WO_4 pairs in the orientationally disordered state in the $Zr_{1-x}M_xW_2O_{8-y}$ system [7].

The normalized phase transition temperatures, $\{T_{trs}$-$(Zr_{1-x}M_xW_2O_{8-y})/T_{trs}(ZrW_2O_8)\}$, of $Zr_{1-x}Lu_xW_2O_{8-y}$ are plotted against their saturated order parameters in Fig. 8 together with those of $Zr_{1-x}M_xW_2O_{8-y}$ (M = Sc, Y, In) reported in our previous study [7]. In the $Zr_{1-x}M_xW_2O_{8-y}$ (M = Sc, Y, In) system, the phase transition temperatures were
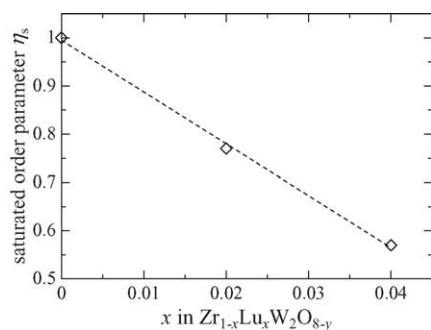

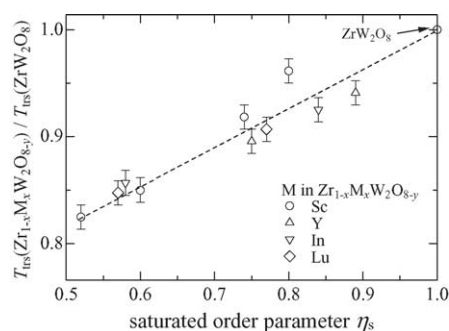Fig. 7. Saturated order parameter of $Zr_{1-x}Lu_xW_2O_{8-y}$ ($x = 0$, 0.02, 0.04) against Lu content.

Fig. 8. Normalized order–disorder phase transition temperatures of $Zr_{1-x}M_xW_2O_{8-y}$ (M = Sc, Y, In, Lu) plotted against their saturated order parameters [7].

in proportion to the saturated order parameter and were on a universal line [7]. The points of $Zr_{1-x}Lu_xW_2O_{8-y}$ were also on the universal line. Therefore, the effect of the Lu-substitution on the $Zr_{1-x}Lu_xW_2O_{8-y}$ system can be also understood for rare earth element having 4f electrons by our model previously proposed associated with the existence of a local region including the WO_4 pairs having the orientational disorder [7]. If we assume the local region to form a sphere around the substituted Lu site, it is easy to estimate the size of the local region per one substituted Lu from the lattice parameter, the saturated order parameter and the Lu content. The averaged radius of the local region was estimated to be about 1.6 nm in $Zr_{1-x}Lu_xW_2O_{8-y}$ at 121 K. This value is intermediate between $Zr_{1-x}Sc_xW_2O_{8-y}$ and $Zr_{1-x}In_xW_2O_{8-y}$ [7]. The volume of the spherical region corresponds to about 2–3 unit cells. The "large" regions play a role of a cluster of nonmagnetic impurities in a site-diluted magnetic system, leading to the drastic lowering of the phase transition temperature in $Zr_{1-x}Lu_xW_2O_{8-y}$ with just a few percent in Lu content. The investigation on $Zr_{1-x}M_xW_2O_{8-y}$ substituted by lanthanoid elements having smaller atomic number than Lu is in progress to confirm the wide applicability of the present model.

4. Conclusions

$Zr_{1-x}Lu_xW_2O_{8-y}$ solid solutions substituted by rare earth element having 4f electrons were newly synthesized successfully. The soluble range was at least up to $x = 0.04$. The phase transition temperatures, T_{trs}, and the saturated order parameters, η_s, in $Zr_{1-x}Lu_xW_2O_{8-y}$ decreased linearly with increasing Lu content. The linear relation between T_{trs} and η_s in $Zr_{1-x}Lu_xW_2O_{8-y}$ agreed well with those of $Zr_{1-x}M_xW_2O_{8-y}$ (M = Sc, Y, In). It was concluded that our proposed model to explain the effect of the substitution by the trivalent cation was also applicable to $Zr_{1-x}Lu_xW_2O_{8-y}$ substituted by rare earth element.

References

[1] T.A. Mary, J.S.O. Evans, T. Vogt, A.W. Sleight, Science 272 (1996) 90.

[2] J.S.O. Evans, T.A. Mary, T. Vogt, M.A. Subramanian, A.W. Sleight, Chem. Mater. 8 (1996) 2809.

[3] Y. Yamamura, N. Nakajima, T. Tsuji, Solid State Commun. 114 (2000) 453.

[4] Y. Yamamura, N. Nakajima, T. Tsuji, Phys. Rev. B 64 (2001) 184109.

[5] J.S.O. Evans, W.I.F. David, A.W. Sleight, Acta Crystallogr. B 55 (1999) 333.

[6] N. Nakajima, Y. Yamamura, T. Tsuji, Solid State Commun. 128 (2003) 193.

[7] Y. Yamamura, N. Nakajima, T. Tsuji, A. Kojima, Y. Kuroiwa, A. Sawada, S. Aoyagi, H. Kasatani, Phys. Rev. B 70 (2004) 104107.

[8] T. Tsuji, Y. Yamamura, N. Nakajima, Thermochim. Acta 416 (2004) 93.

[9] J.B. Nelson, D.P. Riley, Proc. Phys. Soc. London 57 (1945) 160.

[10] R.D. Shannon, Acta Crystallogr. A 32 (1976) 751.

[11] Y. Yamamura, T. Tsuji, K. Saito, M. Sorai, J. Chem. Thermodyn. 36 (2004) 525.